Eur Biophys J (1998) 27: 638–645

ARTICLE

J. Fitter · O. P. Ernst · T. Hauß · R. E. Lechner
K. P. Hofmann · N. A. Dencher

Molecular motions and hydration of purple membranes and disk membranes studied by neutron scattering

Received: 12 February 1998 / Revised version: 18 March 1998 / Accepted: 27 March 1998

Abstract Fast stochastic equilibrium fluctuations (time scale: 10^{-10}–10^{-13} seconds) in purple membranes (PM) and in disk membranes (DM) have been measured with quasielastic incoherent neutron scattering. The comparison of predominantly stochastic motions occurring in purple membranes and in disk membranes revealed qualitatively similar dynamical behaviour. Models of internal motions within restricted volumes have been shown to be useful to fit the spectra from both samples. From fits using these models we found "amplitudes" 15 to 20% larger for motions in DM samples compared to PM samples. This indicates a higher internal flexibility of the DM. Because the dynamical behaviour is very sensitive to the hydration of the protein-lipid complex, we also performed neutron diffraction experiments to determine lamellar spacings as a measure of level of hydration and as a function of temperature. From these studies the interaction of solvent molecules with the surface of the protein-lipid complex appears to be qualitatively similar for both types of membranes.

Key words Purple membrane · Disk membrane · Quasielastic incoherent neutron scattering · Lamellar structure · Diffusive motions

Based on a presentation at the 2nd European Biophysics Congress, Orléans, France, July 1997

J. Fitter (✉)
Forschungszentrum Jülich, IBI-2, Biologische Strukturforschung, D-52425 Jülich, Germany
e-mail: j.fitter@fz-juelich.de

J. Fitter · T. Hauß · R. E. Lechner
Hahn-Meitner-Institut, BENSC, Glienicker Strasse 100, D-14109 Berlin, Germany

J. Fitter · T. Hauß · N. A. Dencher
Institut für Biochemie, TU Darmstadt, Petersenstrasse 22, D-64287 Darmstadt, Germany

O. P. Ernst · K. P. Hofmann
Institut für medizinische Physik und Biophysik, Medinizische Fakultät, Humboldt-Universität, Charité, Ziegelstrasse 5–9, D-10098 Berlin, Germany

1 Introduction

One of the main features of biological macromolecules is their individual and specific three dimensional structure. In the case of proteins this feature is more or less determined by the sequence of the amino acids. On the other hand, the physiological function of proteins cannot be completely understood from their static structures since dynamical aspects are of great importance. Internal molecular motions, which give biological molecules the conformational flexibility required for function have been studied by Mössbauer spectroscopy, NMR techniques, neutron spectroscopy, and molecular dynamic simulations (for an overview see, for example, McCammon and Harvey 1987). In particular, studies using neutron scattering techniques (time scale 10^{-10}–10^{-13} seconds) revealed that environmental conditions (e.g., hydration, temperature) have a strong influence on the dynamical behaviour (Doster et al. 1989; Ferrand et al. 1993; Andreani et al. 1995; Fitter et al. 1996a, b). In these studies water soluble proteins (myoglobin, superoxide dismutase) as well as the integral membrane protein bacteriorhodopsin have been investigated. Qualitatively all these proteins exhibit the same main features: (i) decreasing flexibility as represented by internal motions on the picosecond time scale, when the temperature and the hydration level are lowered. (ii) Dynamical transition accompanied by the onset of nonharmonic large amplitude motions, when the temperature is increased beyond about 170 to 230 K.

In the present work we report on a neutron scattering study comparing two membrane proteins embedded in their natural lipids. We have studied the light-driven proton pump bacteriorhodopsin (BR) in the purple membrane (PM) and the photoreceptor rhodopsin (RH) in the disk membrane (DM). Both proteins are integral membrane proteins having a seven-helix membrane-spanning structure with a molecular mass of 27 kD (BR) and about 40 kD (RH). In contrast to the membrane proteins BR and RH, which share many similarities, the whole membranes are very different. The DM is characterized by a much larger

fluidity due to more lipid molecules per RH (≈60 moles lipids/mole RH) as compared to the PM, where BR forms a more rigid complex, having strong protein-protein interactions, and with only a few lipids (≈8 moles lipids/mole BR) (for more details see, for example, Stoeckenius et al. 1979; Hofmann and Heck 1996). The subject of this work was to study the internal molecular motions by the use of quasielastic incoherent neutron scattering (QINS). As already mentioned above, the hydration of biological macromolecules is of great importance for function, because essential dynamical properties are very sensitive to the level of hydration. Using lamellar structures, like stacks of membrane sheets, enables one to study important properties of the hydration water. Therefore, we have also performed neutron diffraction experiments at different temperatures, in order to analyse solvent properties which are directly related to the dynamical behaviour.

2 Sample preparation

Purple membranes. Patches of purple membranes were isolated from *Halobacterium salinarum* according to standard procedures (Bauer et al. 1976). The patches obtained (patch diameter of about 0.5–1.0 µm) were washed with distilled D_2O. By a slow drying process of a suspension (6 ml) with 200 mg PM, we obtained oriented stacks with membrane planes parallel to a planar sample support (aluminum plates: thickness 0.2 mm, diameter of 50 mm).

Disk membranes. Bovine rod outer segments (ROS) were prepared according to Wilden and Kühn (1982) from fresh, dark-adapted retinas obtained from a local slaughterhouse by means of a discontinuous sucrose density gradient centrifugation. All procedures were performed under dim red light. To obtain washed disk membranes, peripheral proteins were fivefold extracted from the ROS preparation with extraction buffer (5 mM Pipes, 1 mM EDTA, 1 mM DTT, pH 7.0) followed by centrifugation. The membranes were washed with 5 mM Bis-Tris, 200 mM NaCl, pH 6.2 in deionized water and then with 5 mM Bis-Tris, 500 mM NaCl, pH 6.2 in D_2O. The pellet was resuspended by vortexing, briefly ultrasonicated and sedimented for 6 hrs at 4500 g and 15 °C (K80 centrifuge, VEB MLW Medizintechnik Leipzig, former GDR) onto aluminum plates. In order to reduce the high salt concentrations after centrifugation, the pellet was briefly washed by twofold immersion in 5 mM Bis-Tris (pH 6.2) in D_2O. Finally, an amount of 250 mg disk membrane patches (with a diameter less than 1.5 µm) was dried under controlled conditions.

Preparation of hydrated membrane stacks. Owing to the drying process of the membrane suspensions we obtained samples, consisting of lamellar stacks with membranes parallel to the surface of the aluminum plates. Neutron scattering experiments require a large amount of sample material, at least 100–200 mg. In this case, a reproducible adjustment of a specific hydration level needs a rather long equilibrium time. Both types of sample have been rehydrated with D_2O using vapor exchange over a saturated K_2SO_4 solution (corresponding to a relative humidity of 98% at 20 °C) within an exsiccator. The corresponding hydration levels have been monitored by measuring the lamellar spacings and by the determination of sample weight. After approximately seven days, final (equilibrium) hydration levels have been reached with h = 0.51 g D_2O per g membranes for the DM and with h = 0.42 for the PM[1]. In addition to these hydration levels, dried DM and PM samples were prepared for neutron diffraction experiments. These samples have been dried by exposing them for three days to silica gel within the exsiccator. All samples were sealed in circular slab-shaped aluminum containers, which guaranteed constant water content during the experiments.

3 Measurements and data analysis

3.1 Neutron diffraction

Lamellar diffraction patterns were recorded in so-called $\omega,2\theta$ scans with wavelengths of 5.418 Å and 4.617 Å using the V1 Membrane-diffractometer at the Hahn-Meitner Institut (Berlin). Sample temperatures between 220 and 300 K were set using an "orange"-cryostat (ILL standard type). The measurements have been performed by cooling the samples from 300 K down to 220 K, applying a cooling rate of approximately 8 K per hour. Subsequently the samples were heated with a rate, which was also about 8 K per hour. Excitation of lamellar reflections was obtained by the use of a sample orientation, where the vertical surface of the slab-shaped sample was nearly parallel to the incoming beam direction. In $\omega,2\theta$-scans we measured first (and in some cases second) order reflections on a two-dimensional position sensitive ^{3}He-detector. Owing to the fact that the samples were hydrated with D_2O, large intensities were obtained for the lamellar reflections. Therefore, a measuring time of about 10 minutes for each ω position was sufficient to determine 2θ values for the first order reflections. Values of the lamellar spacing were obtained from the 2θ values.

3.2 Time-of-flight spectroscopy

Time-of-flight (TOF) spectra were measured using the high-resolution multichopper spectrometer NEAT (Lechner 1996) located at the Hahn-Meitner Institut. Using incident wavelengths of 6.20 Å and 5.10 Å, elastic energy

[1] A direct comparison of h-values between PM and DM is not straightforward, because the PM and the DM have different membrane thicknesses, different protein-lipid ratios and therefore different specific densities (see Sect. 4.1 and Table 1)

Table 1 Distribution of protons in the purple membrane and in the disk membrane as calculated from membrane compositions determined by Kates et al. (1982), Ovchinichov et al. (1979), Miljanich et al. (1981) and Hargrave et al. (1983)

Composition	Purple membrane		Disk membrane	
	Content (w/w) [%]	Number of nonexchangeable protons (per BR-molecule)	Content (w/w) [%]	Number of nonexchangeable protons (per RH-molecule)
BR	75	1891	–	–
RH	–	–	45	2619
Lipids	25	635	50	3621
Other proteins	–	–	5	131*
Total	100	2526	100	6371

* This number was approximated by the assumption, that other proteins in the DM have the same number of nonexchangeable protons per molecular mass as rhodopsin

resolutions ΔE of 34 μeV and 100 μeV (FWHM) within an angular range of $13.3° \leq \phi \leq 136.7°$ were achieved. Both samples, which have been measured at room temperature (293 K), exhibit transmission values of T (90°) = 0.92–0.94. A sample orientation angle of $\alpha = 45°$ with respect to the incident neutron beam direction was used for all samples, including vanadium standard and empty can. This sample orientation guaranteed that no Bragg reflections are excited and the predominant part of the measured signal is due to incoherent neutron scattering from nonexchangeable hydrogen atoms. All TOF spectra were corrected, normalized, grouped and transformed to the energy transfer scale using the data analysing program FITMO (Fitter 1998). A correction for multiple scattering has not been applied.

The incoherent scattering from quasi-homogenously distributed nonexchangeable hydrogen atoms in the biological macromolecules gives information on the general dynamical properties of these molecules. According to the formalism of the self correlation functions developed by Van Hove (1954) the incoherent scattering function $S_{\mathrm{inc}}(\boldsymbol{Q}, \omega)$ can be related to the self correlation function $G_s(\boldsymbol{r}, t)$:

$$S_{\mathrm{inc}}(\boldsymbol{Q}, \omega) = \frac{1}{2\pi} \int_{-\infty}^{\infty} \mathrm{e}^{-i\omega t} \int_{-\infty}^{\infty} \mathrm{e}^{\boldsymbol{Q}\boldsymbol{r}} \cdot G_{\mathrm{s}}(\boldsymbol{r}, t)\, d\boldsymbol{r}\, dt \qquad (1)$$

In the classical approximation the Fourier transform in space and time of the incoherent scattering function $G_s(\boldsymbol{r}, t)$ describes the average time dependent probability density distribution of hydrogen atoms (see for example Lechner 1983). $G_s(\boldsymbol{r}, t)$ may be found as a solution of an equation of motion describing the dynamics of all hydrogen atoms. Because our samples include many hydrogen atoms located in very different environments (see Table 1), it is in general not straightforward to find an adequate equation of motion. Therefore we use simple models, which should describe some general properties of the complex dynamical behaviour as found in biomolecules. According to the stochastic character of the predominant part of the motions, a sum of Lorentzians was used to describe the theoretical scattering function

$$S_{\mathrm{theor}}(\boldsymbol{Q}, \omega) = e^{-\langle u^2 \rangle Q^2} \cdot \left[A_0(\boldsymbol{Q}) \cdot \delta(\omega) + \sum_n A_n(\boldsymbol{Q}) \cdot L_n(H_n, \omega) \right] \qquad (2)$$

Here the scattered intensity was separated into an elastic $\delta(\omega)$-shaped component and quasielastic Lorentzian-shaped contributions $L_n(H_n, \omega)$, where $H_n = (\tau_n)^{-1}$ are the widths (HWHM) of the Lorentzians (τ_n are the corresponding correlation times). The intensity fractions corresponding to these components are described by the elastic incoherent structure factor (A_0 or EISF) and the quasielastic incoherent structure factors (A_n). The inelastic spectral contributions have been taken into account by the Debye-Waller factor, where $\langle u^2 \rangle$ gives the global average "mean square displacement" of vibrational motions. The theoretical scattering function was fitted to the measured $S_{\mathrm{meas}}(\boldsymbol{Q}, \omega)$ scattering function:

$$S_{\mathrm{meas}}(\boldsymbol{Q}, \omega) = F_N \cdot e^{\frac{-h\omega}{2k_B T}} \cdot \left[S_{\mathrm{theor}}(\boldsymbol{Q}, \omega) \otimes S_{\mathrm{res}}(\boldsymbol{Q}, \omega) \right] + B \qquad (3)$$

In addition to the scalar quantities, such as the normalisation factor F_N, linear "background" B, and the detailed balance factor $e^{\frac{-h\omega}{2k_B T}}$ a convolution (⊗: energy convolution operation) with the resolution function $S_{\mathrm{res}}(\boldsymbol{Q}, \omega)$ obtained from vanadium measurements has been applied.

4 Results and discussion

4.1 Lamellar structure and hydration

Because the samples were made of alternating layers of solvent water molecules and membrane sheets giving them the character of lamellar structures we were also able to study aspects of the solvent-membrane interaction by measuring lamellar spacings. Measurements with dried samples gave lamellar spacings which correspond to the thickness of the sole membrane. With increasing hydration level one obtains larger values of the lamellar spacing, which include the thickness of the water layers between two adjacent membrane bilayers. Recent measurements of the lamellar spacings of hydrated PM stacks as a function of temperature have shown that the membranes are partially dehydrated, when cooled below a hydration water freezing point T_{fh} (Fig. 1). This phenomenon is reversible, and a hysteresis is observed, when the PM is rehyrated upon reheating. In several measurements using cooling/heating rates from 5 to 40 K per hour, we did not observe any rate dependence. Therefore, we were certain that at every temperature of these measurements the sample was practically at thermal equilibrium (Lechner et al. 1998). We have now carried out such measurements on DM and compare the results to those of PM.

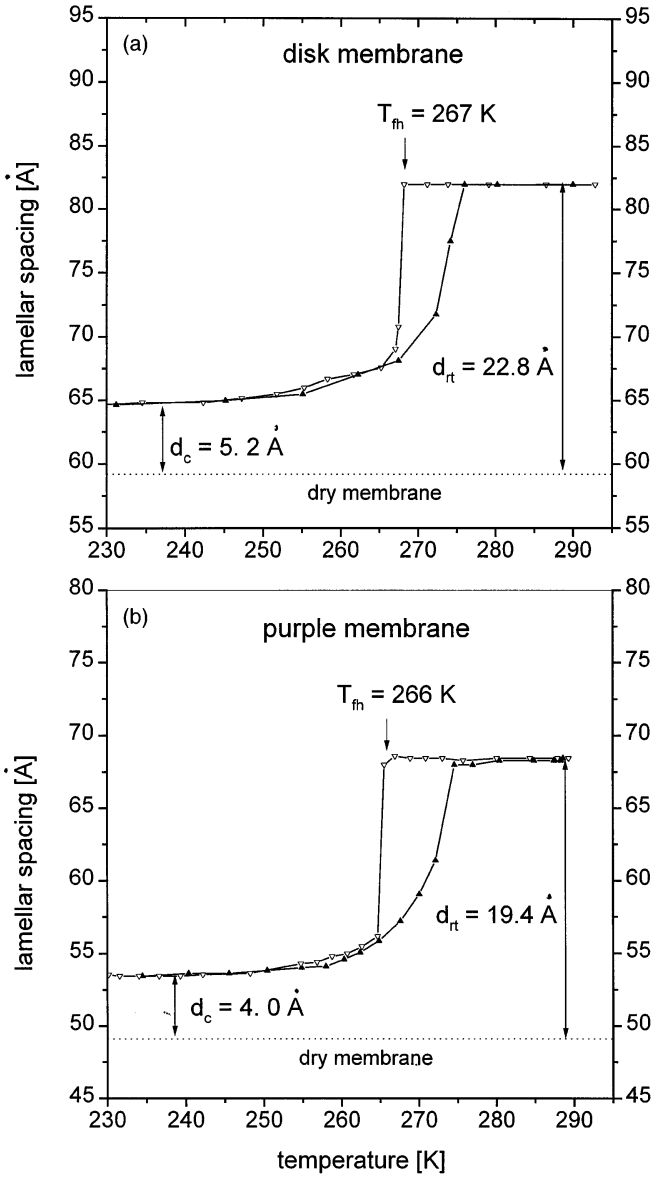

Fig. 1a, b Lamellar spacings of hydrated disk membrane and purple membrane samples measured as a function of temperature (cooling: *downsided triangles*; heating: *upsided triangles*). In order to obtain the water layer thickness (at room temperature: d_{rt}; below 240 K: d_c), lamellar spacings of dried samples have been measured. Because these values do not show a temperature dependence (see Lechner et al. 1998), they are represented by a straight *dotted line*

(i) Comparing the lamellar spacings from PM and DM samples we find much larger values for the DM samples (Fig. 1). This is certainly due to the fact that rhodopsin is a larger molecule than BR, with much larger loop regions protruding in the intermembrane space. In addition, hydrophilic oligosaccharides, which are linked to membrane proteins in the DM (Fukuda et al. 1979), protrude into the intermembrane space and may also determine the lamellar spacing. For dried samples we find a membrane thickness (single bilayer) of 59.2 Å for the DM and 49.1 Å in the case of PM (see Fig. 1). These values are in good agreement with values determined in previous studies (Zaccai 1987; Papadopoulos et al. 1990; Dratz et al. 1979; Pascolini et al. 1984). According to a topological model of rhodopsin in DM (Hargrave et al. 1984) it is assumed, that only 50% of the total protein is in the interior of the lipid bilayer, while 25% protrude in the interbilayer space on each side of the membrane. In the case of BR in the PM one finds nearly 80% of the protein embedded in the lipids, whereas only 10% of the protein on each side of the membrane is part of the loop regions (Grigorieff et al. 1996).

(ii) At room temperature and a rather high hydration levels (such as h = 0.42 and 0.51) the predominant part of the solvent molecules is located in the intermembrane space represented by the corresponding water layer thickness, given in Fig. 1, of d_{rt}: 19.4 Å (PM), 22.8 Å (DM). At the freezing temperature T_{fh} a significant part of the solvent suddenly starts to crystallize, accompanied by a tremendous decrease of lamellar spacings indicating a "removal" of solvent molecules out of the interbilayer space. Well below the freezing point we find in both types of membranes a limited amount of nonfreezing water, corresponding to a thickness d_c of about 2 monolayers of water, that is bound quite tightly to the membrane surface (Lechner et al. 1998).

The purple membrane and the disk membrane are characterized by very different protein-lipid ratios and different kinds of lipids and proteins with possibly different membrane surface charges. This might be the reason that we observe differences in the d_{rt} and d_c values. Nevertheless, the interaction with solvent molecules (characterized for instance by T_{fh} and d_c) is qualitatively similar (Fig. 1). With respect to the dynamical behaviour of the protein-lipid complex one may therefore expect that the influence of the solvent on the dynamics of the different molecules in the membrane (lipids and proteins) is also qualitatively similar for both types of membrane.

4.2 Dynamical behaviour

As known from previous work, the observed motions on the picosecond time scale are mainly stochastic reorientations of molecular subunits, such as polypeptide side groups or fatty acid chains (Fitter et al. 1996b; König et al. 1995). We applied two simple models, which can be used to describe these local diffusive motions within restricted volumes.

Jump diffusion between two sites: The simplest model for a motion is a jump between two separated sites. Such a motion is parameterized by a jump distance d, which can be for example the distance between two potential minima. A spatial average over all possible orientations of d leads to

$$A_0(\boldsymbol{Q}) = \frac{1}{2}\cdot\left[1+\frac{\sin(Q\,d)}{Q\,d}\right] \tag{4}$$

for the elastic incoherent structure factor (EISF) (see for example Lechner et al. 1983). Here the jump distance d permits a description of the "volume" available for this motion.

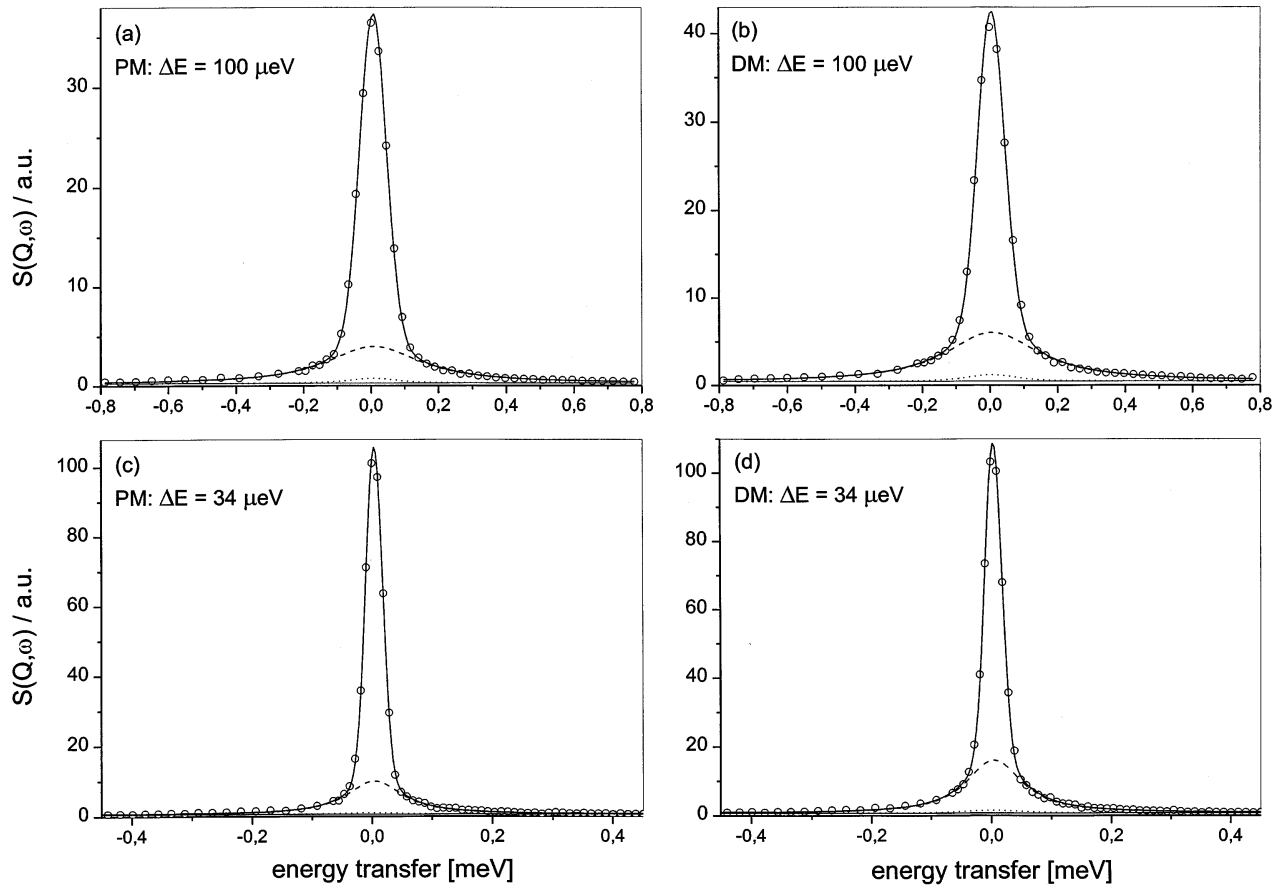

Fig. 2a–d Fits of spectra measured at a scattering angle of $\phi = 90.5°$ with samples of disk membranes (DM) and of purple membranes (PM) are shown in this figure. These spectra have been measured using a wavelength of $\lambda = 5.1$ Å (**a**, **b**) and $\lambda = 6.2$ Å (**c**, **d**), corresponding to an elastic energy resolution of $\Delta E = 100$ μeV and 34 μeV, respectively. The total scattering function which fits the experimental points (*circles*), is composed of an elastic component and two quasielastic components: a Lorentzian corresponding to the internal diffusive motions of the membrane with linewidths of $H = 150$ μeV (**a**, **b**) and 60 μeV (**c**, **d**), represented by *dashed lines*, and one component taking into account solvent scattering with $H = 60$ μeV (*dotted line*). A further straight *solid line* represents a linear background

Diffusion inside a sphere: This model, developed by Volino and Dianoux (1980), is characterized by a free diffusion inside the volume of a sphere with radius *r* and gives an EISF, which is

$$A_0(\boldsymbol{Q}) = \left[3 \frac{\sin(Qr) - Qr \cdot \cos(Qr)}{(Qr)^3} \right]^2 . \qquad (5)$$

Both kinds of model have already been applied in previous work to fit neutron scattering data measured with proteins. The two-site model was used in the case of myoglobin (Doster et al. 1989) and purple membranes (Fitter et al. 1996b), the spherical diffusion model for C-phycocyanin (Bellissent-Funel et al. 1996) and for phosphoglycerate kinase (Receveur et al. 1997). Because our data is limited in *Q* and we used only a restricted energy transfer range, $Q_{max} = 1.85$ Å^{-1} and $|\hbar\omega| \leq 0.5$ meV for the 6.2 Å data, resp. $Q_{max} = 2.25$ Å^{-1} and $|\hbar\omega| \leq 0.8$ meV for data measured with $\lambda = 5.1$ Å, we need to consider only the first quasielastic component, with a width $(\tau_1)^{-1}$ (see for example Bee 1988). Therefore, in the case of both models, we obtain the quasielastic incoherent structure factor (QISF) simply by

$$A_1 = 1 - A_0 . \qquad (6)$$

Since the various moving groups in the samples are structurally different from each other, correlation times τ_1, jump distances *d* and radii *r* must be understood as values averaged over the motions observable in the time window corresponding to the energy resolutions used in the experiments. For samples hydrated in D_2O the major part, approximately 95% (at the given hydration levels), of the scattered intensity is caused by nonexchangeable hydrogens of the membranes. Referring to earlier work, where we have studied the scattering from solvent molecules in purple membranes, we approximate the scattering from D_2O solvent molecules by an additional Lorentzian ($H = 60$ μeV), representing rotational diffusion of solvent molecules (for details see, Lechner et al. 1994a, b and Fitter et al. 1996b). At the given energy resolutions a translational diffusion of solvent molecules appears only as elastic scattering. The *Q* dependent structure factors have been calculated using the theories described in the above mentioned publication and were finally multiplied by a factor $F_{sol} = h \cdot SP_D$ (*h*: hydration level, $SP_D = 1/11$ scatter-

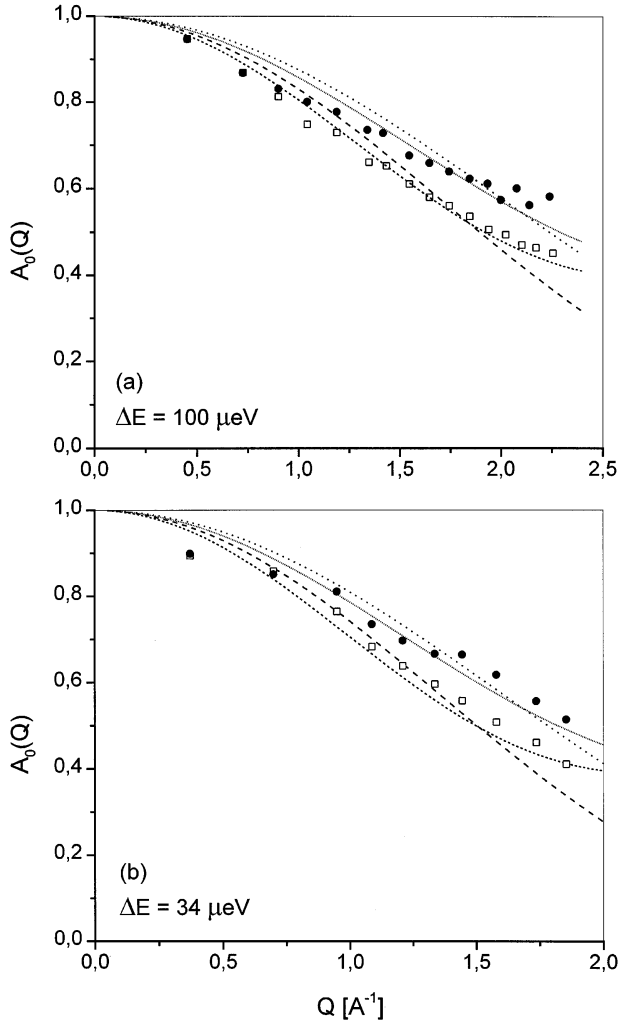

Fig. 3a, b *Q*-dependence of EISF. For the 5.1 Å data (**a**) and the 6.2 Å data (**b**) the experimental EISF (or A_0) as obtained from "free fits" of DM spectra (*open squares*) and of PM spectra (*solid circles*) are shown as a function of *Q*. These fits have been performed for each spectrum separately with radius *r* (or jump distances *d*) as a free parameter. The statistical error of the experimental EISF is approximately ±0.015, which is about the size of the symbols. The corresponding theoretical EISF were obtained from a fit, where all spectra of a data set have been fitted simultaneously. For the "2-site jump" model and the "diffusion in a sphere" model they are represented by the following lines: "2-site jump" model: PM (*short dotted*), DM (*short dashed*); "diffusion in a sphere" model: PM (*long dotted*), DM (*long dashed*). The resulting jump distances and radii are given in Table 2

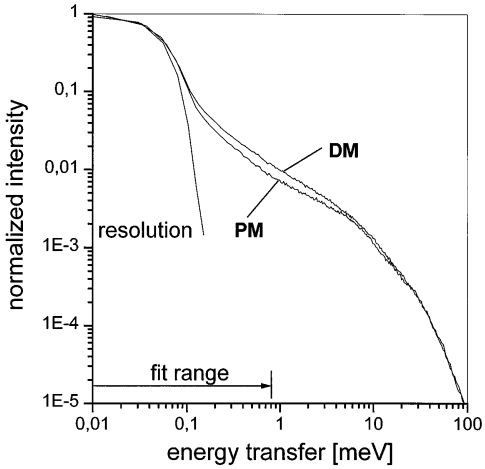

Fig. 4 "log-log" plot of the 5.1 Å data. For PM and DM the data shown represent the sum over spectra measured at all scattering angles ϕ = 13.3°–136.7°

ing power of deuterons compared to that of hydrogens). For the solvent molecules the resulting incoherent structure factors, as well as the linewidth of the quasielastic component were represented by fixed parameter values in the fitting procedure.

Model fits using the linewidth τ_1 and the jump distance *d* or radius *r* as free fitting parameters revealed the following results:

(i) Fits of spectra from both samples (PM and DM) give fitting results of acceptable quality for both models (Figs. 2 and 3). As predicted in the theory of diffusion in restricted volumes the linewidth obtained is *Q* independent.

(ii) Because we used two data sets with different energy resolutions and different energy transfer ranges we obtained different linewidths for both data sets. For the data measured with an energy resolution of 34 μeV (6.2 Å data) we obtained a linewidth of 60 μeV corresponding to a correlation time of τ_1 = 11.0 ps. In the case of data measured with 100 μeV energy resolution (5.1 Å data) as linewidth of 150 μeV with a corresponding correlation time of τ_1 = 4.4 ps has been obtained.

(iii) As seen in Fig. 3 larger EISF values found in the case of PM samples, indicate a smaller internal flexibility as compared to DM samples. This behaviour is observed in both data sets.

The extent to which qualitative agreement of experimental EISF with theoretical values is obtained for both models, is shown in Fig. 3. For both models we found systematic deviations from theoretical *Q* dependence of the EISF at low *Q* values, which are typical for multiple scattering effects (see for example Steiner et al. 1991). In the *Q* range up to approximately 1.5–1.7 $Å^{-1}$ both models show a very similar *Q* dependence of the EISF. Above this *Q* value the EISF values are larger in the case of the "2-site jump" owing to the smaller number of accessible states as compared to the "diffusion in a sphere" model. With respect to the experimental data from higher *Q* values (Q = 1.7–2.25 $Å^{-1}$), we observe a slightly better agreement with the "2-site jump" model. This appears to be plausible, given the fact that mobile side groups cannot rotate isotropically because of necessarily existing geometric restrictions. Because our experimental data is limited in *Q* (Q_{max} = 1.85 $Å^{-1}$ and 2.25 $Å^{-1}$) we can at present not go beyond this qualitative statement. Furthermore one has to consider, that these simple models can only be a crude approximation of a much more complex dynamical behaviour, which might also lead to systematic deviations at higher *Q* values (above Q = 2.5 $Å^{-1}$). Nevertheless, these

Table 2 The resulting jump distances and radii (standard deviation 0.017 Å) are given for model fits of the 5.1 Å data with the corresponding 150 μeV component and for the 6.2 Å data represented by a 60 μeV component (for more details, see text)

Model	Purple membrane		Disk membrane	
	Quasielastic component H = 60 μeV [τ = 11.0 ps]	Quasielastic component H = 150 μeV [τ = 4.4 ps]	Quasielastic component H = 60 μeV [τ = 11.0 ps]	Quasielastic component H = 150 μeV [τ = 4.4 ps]
2-site jump diffusion with jump distance d [Å]	1.72	1.37	2.10	1.63
Diffusion inside a sphere with radius r [Å]	1.02	0.81	1.21	0.96

models are good enough to perform a qualitative comparison of the different samples. The reduced internal flexibility of moving H atoms in the PM as compared to the DM, is expressed by smaller values of jump distances ad radii, as shown in Table 2. Compared to the 4.4 ps component we find larger "amplitudes" in both samples for the slower 11.0 ps component. Although the absolute values for the amplitudes of motions are strongly dependent on the geometry of the motion (i.e., the specific model), the relation of radii or jump distances from both samples is the same for both models. We always find jump distances or radii obtained from the PM sample which are approximately 80–85% of those obtained from the DM sample.

In addition to the analysis of the quasielastic components we also compared the contributions of scattered intensity at higher energy transfers in a "log-log" plot (Fig. 4). This figure shows not only (quasielastic) scattering related to motions in the picosecond time range, but also (inelastic) scattering, which is due to vibrational motions (in this figure up to 100 meV, corresponding to τ = 6.6 femtoseconds). As already shown for the diffusive motions, the vibrational motions exhibit a larger contribution in the DM samples as compared to the PM samples. Above approximately 3 mev ($\tau \sim$ 0.2 ps) the difference becomes small.

In such complex systems as the PM and the DM, it is not easy or straightforward to find out the origin of the observed differences in the dynamical behaviour. In particular, we are not able to decide whether the differences in the dynamical behaviour are related to the proteins (BR and RH). Including results from a previous study on different kinds of PM samples indicates that the amount of lipids in the membranes plays a major role in the dynamical behaviour. In this recently published study we reported on a comparison of dynamics in delipidated (5% lipid, 95% protein) and natural (25% lipid, 75% protein, see Table 1) PM samples (Fitter et al. 1997). As a result of this comparison, we found more internal flexibility in the natural PM as compared to delipidated PM samples. Supporting the conclusion that more lipids increase the internal flexibility of a protein-lipid complex, "amplitudes" of internal motion have been obtained from delipidated PM samples, which were only 75%–85% of those obtained from the natural PM (Fitter et al., unpublished results). Interestingly, a comparison of all three samples revealed, that the "amplitudes" (delipidated PM: d = 1.10 Å, natural PM: d = 1.37 Å, DM: d = 1.63 Å) exhibit, to a very good approximation, a linear dependence on the weight percentage of lipids in the different samples (delipidated PM: 5%, natural PM: 25%, DM: 50%). Therefore, the different protein-lipid ratios of PM and DM might be the predominant reason for the observed differences in the dynamics. In this case, differences in the dynamical behaviour between BR and RH which might exist due to differences in the structure (e.g., larger loop regions in RH as compared to BR), could to be small. Otherwise, one would expect clearly larger differences in the scattering between DM and natural PM as compared to delipidated PM and natural PM.

Acknowledgements We thank the technical staff at the Hahn-Meitner Institut for their assistance, Mrs. C. Schröpfer (TU Darmstadt) was well as C. Koch (Humboldt-Universität Berlin) for preparing purple membranes and disk membranes, respectively. This work was supported by grants from the Deutsche Forschungsgemeinschaft (SFB 472 and 366), from the Bundesministerium für Bildung und Forschung (03-DE4DAR-1) and by Fonds der Chemischen Industrie (to N.A.D.).

References

Andreani C, Filabozzi A, Menzinger F, Desideri A, Deriu A, Di Cola D (1995) Dynamics of hydrogen atoms in superoxide dismutase by quasielastic neutron scattering. Biophys J 68: 2519–2523

Bee M (1988) Quasielastic neutron scattering. Adam and Hilger, Philadelphia

Bellisent-Funel M-C, Zanotti J-M, Chen SH (1996) Slow dynamics of water molecules on the surface of a globular protein. Faraday Discuss 103: 281–284

Bauer PJ, Dencher NA, Heyn M (1976) Evidence for chromophore interactions in the purple membrane from reconstitution experiments of chromophore-free membrane. Biophys Struct Mechanism 2: 79–92

Cusack S, Doster W (1990) Temperature dependence of low frequency dynamics of myoglobin. Biophys J 58: 243–251

Doster W, Cusack S, Petry W (1989) Dynamical transition of myoglobin revealed by inelastic neutron scattering. Nature 337: 754–756

Dratz EA, Miljanich GP, Menes PP, Gaw JE, Schwartz S (1979) The structure of rhodopsin and its disposition in the rod outer segments disk membrane. Photochem Photobiol 29: 661–670

Ferrand M, Dianoux AJ, Petry W, Zaccai G (1993) Thermal motions and function of bacteriorhodopsin in purple membranes: effects of temperature and hydration studied by neutron scattering. Proc Natl Acad Sci USA 90: 9668–9672

Fitter J, Lechner RE, Büldt G, Dencher NA (1996a) Temperature dependence of molecular motions in the membrane protein bacteriorhodopsin from QINS. Physica B 226: 61–65

Fitter J, Lechner RE, Büldt G, Dencher NA (1996b) Internal molecular motions of bacteriorhodopsin: hydration-induced flexibility studied by quasielastic incoherent neutron scattering using oriented purple membranes. Proc Natl Acad Sci USA 93: 7600–7605

Fitter J, Lechner RE, Dencher NA (1997a) Influence of lipids on the dynamical behavior of bacteriorhodopsin in the purple membrane. In: Cusack S, Buettner H, Ferrand M, Langan P, Timmins P (eds) Biological macromolecular dynamics. Adenine Press, New York, pp 123–127

Fitter J, Lechner RE, Dencher NA (1997b) Picosecond molecular motions in bacteriorhodopsin from neutron scattering. Biophys J 73: 2126–2137

Fitter J (1998) TOF-data analysing program for NEAT. Interner Bericht, Hahn-Meitner-Institut, Berlin

Fukuda MN, Papermaster DS, Hargrave PA (1979) Rhodopsin carbohydrate: Structure of small oligosaccharides attached at two sites near the NH_2 terminus. J Biol Chem 254: 8201–8207

Grigorieff N, Ceska TA, Downing KH, Baldwin JM, Henderson R (1996) Electron-crystallographic refinement of the structure of bacteriorhodopsin. J Mol Biol 259: 393–421

Hargrave PA, McDowell JH, Curtis DR, Wang JK, Juszcak E, Fong SL, Rao JKM, Smith DP (1983) Structure of bovine rhodopsin. Biophys Struct Mech 9: 235–244

Hofmann KP, Heck M (1996) Light-induced protein-protein interactions of the rod photoreceptor disc membrane. Biomembrane 2A: 141–198

Kates M, Kushwaha SC, Sprott GD (1982) Lipids of purple membrane from extreme halophiles and methanogenic bacteria. Methods Enzymol 88: 89–111

König S, Bayerl TM, Coddens G, Richter D, Sackmann E (1995) Hydration dependence of chain dynamics and local diffusion in L-α-dipalmitoylphosphatidylcholine multilayers studied by incoherent quasielastic neutron scattering. Biophys J 68: 1871–1880

Lechner RE (1983) Neutron scattering studies of diffusion in solids. In: Beniere F, Catlow CRA (eds) Mass transport in solids. Plenum Press, pp 169–226

Lechner RE, Dencher NA, Fitter J, Büldt G, Belushkin AV (1994a) Proton diffusion on purple membrane studied by neutron scattering. Biophys Chem 49: 91–99

Lechner RE, Dencher NA, Fitter J, Dippel T (1994b) Two-dimensional proton diffusion on purple membrane. Solid State Ionics 70/71: 296–304

Lechner RE (1996) NEAT experiments at BENSC. Neutron news 7: 9–11

Lechner RE, Fitter J, Dencher NA, Hauß T (1998) Dehydration of biological membranes by cooling: an investigation on the purple membrane. J Mol Biol 277: 593–603

McCommon JA, Harvey SC (1987) Dynamics of proteins and nucleic acids. Cambridge University Press, Cambridge

Miljanich GP, Nemes PP, White DL, Dratz EA (1981) The asymmetric transmembrane distribution of phosphatidylethanolamine, phosphatidylserine, and fatty acids of bovine retinal rod outer segment disc membrane. J Memb Biol 60: 249–255

Ovchinikov YA, Abdulaev NG, Feigina MY, Kiseley AV, Lobanov NA (1979) The structural basis of functioning of bacteriorhodopsin: an overview. FEBS Lett 100: 219–224

Papadopoulos G, Dencher NA, Zaccai G, Büldt G (1990) Water molecules and exchangeable hydrogen ions at the active centre of bacteriorhopsin localized by neutron diffraction. J Mol Biol 214: 15–19

Pascolini D, Blaise JK, Gruner SM (1984) A 12 Å resolution x-ray diffraction study of the profile structure of isolated bovine retinal rod outer segment disk membranes. Biochim Biophys Acta 777: 9–20

Receveur V, Calmettes P, Smith JC, Desmadril M, Coddens G, Durand D (1997) Picosecond dynamical changes on denaturation of yeast phosphoglycerate kinase revealed by quasielastic neutron scattering. Proteins 28: 380–387

Steiner T, Saenger W, Lechner RE (1991) Dynamics of orientationally disordered hydrogen bonds and of water molecules in a molecular cage. Mol Phys 72: 1211–1232

Stoeckenius W, Lozier RH, Bogomolni RA (1979) Bacteriorhodopsin and the purple membrane of halobacteria. Biochim Biophys Acta 505: 215–278

Van Hove L (1954) Correlations in space and time and born approximation scattering in systems of interacting particles. Phys Rev 95: 249–262

Volino F, Dianoux AJ (1980) Neutron incoherent scattering law for diffusion in a potential of spherical symmetry: general formalism and application to diffusion inside a sphere. Mol Phys 41: 271–279

Wilden U, Kühn H (1982) Light-dependent phosphorylation of rhodopsin: number of phosphorylation sites. Biochemistry 21: 3014–3022

Zaccai G (1987) Structure and hydration of purple membranes in different conditions. J Mol Biol 194: 596–572